

## Novel Oxindole Sulfonamides and Sulfamides: EPZ031686, the First Orally Bioavailable Small Molecule SMYD3 Inhibitor

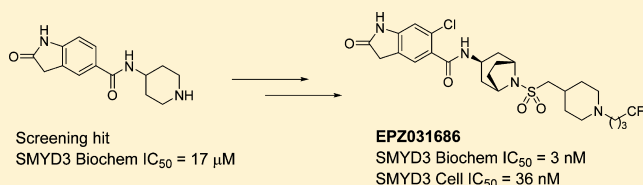
Lorna H. Mitchell,\* P. Ann Boriack-Sjodin, Sherri Smith, Michael Thomenius, Nathalie Rioux, Michael Munchhof, James E. Mills, Christine Klaus, Jennifer Totman, Thomas V. Riera, Alejandra Raimondi, Suzanne L. Jacques, Kip West, Megan Foley, Nigel J. Waters, Kevin W. Kuntz, Tim J. Wigle,<sup>†</sup> Margaret Porter Scott,<sup>‡</sup> Robert A. Copeland, Jesse J. Smith, and Richard Chesworth

Epizyme Inc., Fourth Floor, 400 Technology Square, Cambridge, Massachusetts 02139, United States

## Supporting Information

**ABSTRACT:** SMYD3 has been implicated in a range of cancers; however, until now no potent selective small molecule inhibitors have been available for target validation studies. A novel oxindole series of SMYD3 inhibitors was identified through screening of the Epizyme proprietary histone methyltransferase-biased library. Potency optimization afforded two tool compounds, sulfonamide **EPZ031686** and sulfamide **EPZ030456**, with cellular potency at a level sufficient to probe the *in vitro* biology of SMYD3 inhibition. **EPZ031686** shows good bioavailability following oral dosing in mice making it a suitable tool for potential *in vivo* target validation studies.

**KEYWORDS:** SMYD3, oxindole, methyltransferase, KMT, oncology, tool compound



Set and Mynd Domain containing 3 (SMYD3) is a lysine methyltransferase (KMT) expressed at high levels in a number of different cancer histologies and is associated with a poor clinical prognosis.<sup>1–10</sup> While no single mechanism has emerged to explain this correlation, a number of studies have implicated SMYD3 in the regulation of gene transcription and signal transduction pathways critical for cell survival in breast, liver, prostate, pancreatic, and lung cancer models.<sup>4,7–9</sup>

In addition, considerable evidence has been reported in the literature showing that genetic knockdown of SMYD3 leads to a decrease in proliferation of a variety of cancer cell lines.<sup>4,7–9,11</sup> Two studies, employing RNAi-based technologies, have shown that ablation of SMYD3 in hepatocellular carcinoma cell lines greatly reduces cell viability and that its pro-oncogenic role is dependent on its catalytic activity.<sup>7,9</sup> Moreover, SMYD3 has also been shown to be a critical mediator of transformation induced by a KRAS gain-of-function mutation in both pancreatic and lung adenocarcinoma mouse models; these models were likewise dependent on the catalytic activity of SMYD3.<sup>11</sup>

The biological function of SMYD3 is still poorly understood. Early studies of SMYD3 suggested that its primary function is to methylate histones. Indeed, several reports have indicated that SMYD3 modifies histone H3 on lysine 4,<sup>9,12</sup> but have also identified a novel modification of histone H4 on lysine 5.<sup>7</sup> The results of these studies have not yet yielded a clear picture of how SMYD3 might be regulating chromatin, but a recent study has strongly implicated SMYD3 as a direct regulator of MAPK pathways in the cytoplasm and not as a regulator of transcription. MAP3K2 (MEKK2) was shown to be trimethylated at lysine 260 by SMYD3. Modification of this residue

leads to enhanced downstream MAPK activation and appears to be critical for mutant KRAS driven oncogenesis.<sup>11</sup>

SMYD3's role in cancer cell line proliferation, its effect on known oncogenic signal transduction pathways, and the association of SMYD3 mRNA expression with aggressive transformed phenotypes make SMYD3 an attractive target for therapeutic intervention. We report here the first potent and selective small molecule inhibitors suitable for target validation studies.

Compound **1** was identified as a micromolar inhibitor of SMYD3 through screening of Epizyme's proprietary histone methyltransferase-biased library. The 1.5 Å resolution crystal structure of **1** was solved in a ternary complex with SMYD3 and SAM and revealed the oxindole headgroup made several hydrophobic and electrostatic interactions with the lysine pocket of SMYD3 (Figure 1). The oxindole carbonyl forms a hydrogen bond to the side chain of Ser202 and is within 2.9 Å of the SAM methyl group. The aromatic ring system forms a  $\pi$ -stacking interaction with Phe183, while the oxindole nitrogen makes water-mediated contacts with the protein. The amide of the linker engages the protein via two hydrogen bonds that could mimic a protein substrate. The piperidine tail of **1**, positioned in the large, solvent filled peptide binding site, engaged a water mediated interaction with the side chain carboxyl of Glu192.

**Special Issue:** Epigenetics

**Received:** July 7, 2015

**Accepted:** August 27, 2015



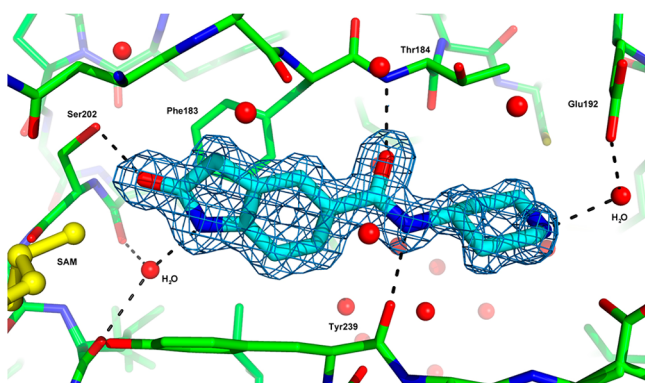


**Figure 1.** Structure of **1** (cyan) in complex with SMYD3 (green) and SAM (yellow) (PDB ID 5CCL). Electron density ( $2F_o - F_c$ ,  $1\sigma$ ) for the compound is shown. Hydrogen bonds are indicated as dashed lines.

Since crystallography revealed that both Glu192 and Asp241 were within 3.5 Å of the piperidine nitrogen of **1** initial design and synthesis of analogues focused on introduction of a basic center in an attempt to interact with one of these acidic residues and boost potency. Indeed, the propylamino-sulfonamide analogue, **2**, was over 10-fold more potent in the biochemical assay than the starting hit, **1**. Introduction of a chlorine group onto the oxindole ring, compound **3**, was tolerated. Constraint of the basic side-chain in the piperidine derivative **4** resulted in a nominal 2-fold potency improvement over the propylamine analogue **2** (Table 1).

Further restriction of conformational freedom with the bridged piperidine core, compound **5**, gave a 17-fold potency improvement over **4**. However, despite the single-digit nanomolar biochemical potency of compound **5** and its chloro-oxindole derivative **6** the cellular activity was still in the micromolar range. This weak cell potency could be attributed to the physicochemical property space of the compounds, in particular the polarity and high number of hydrogen bond donors. This hypothesis is supported by the improvement in cell-to-biochemical shift seen with EPZ031686, which has one of the H-bond donors blocked and increased lipophilicity. EPZ031686 is the first SMYD3 inhibitor identified to show double-digit nanomolar cellular activity.

Decreased biochemical potency was seen when the oxindole NH was methylated in compound **8**, which is not unexpected as this would interrupt the water mediated H-bond interaction to protein observed from this position by crystallography. There is some tolerance in placement of the basic center as the 3-methylpiperidines, **10** and **11**, and the cyclohexylamine **12** retain good biochemical potency (Table 2).

Analogues with sulfamide linkers also showed potent biochemical activity (Table 3). As seen for the sulfonamide series, cellular potency could be improved by blocking H-bond donors, compounds **14** and **15** compared to **13**, and increasing lipophilicity, EPZ030456. The 6-chloro- and 6-fluoro-substituted oxindoles (**13** and **16**) showed similar biochemical potency to the compound with no substitution in this position (**18**).

The two most cell potent compounds, EPZ030456 and EPZ031686, were further characterized. Both compounds showed <30% inhibition against 16 histone methyltransferase targets at a 10 μM screening concentration.<sup>13</sup> Determination of  $IC_{50}$  against the highly homologous SMYD2 enzyme showed both compounds to have  $IC_{50} > 50 \mu M$ .

A crystal structure of EPZ030456 was solved and revealed unambiguous density for the oxindole headgroup, amide sulfamide linker, and piperidine ring, while no density was seen for the terminal benzyl tail (Figure 2). The oxindole groups of **1** and EPZ030456 are superimposable and make all the expected interactions previously described. The main chain of Leu240 and side chains of Met190 and Val368 engage the compound through van der Waals interactions as it spans the width of the peptide binding site. Intriguingly, EPZ030456 binds with low nanomolar affinity although the compound makes few specific interactions with the protein beyond the headgroup and amide linker. Electrostatic and water mediated interactions, unseen in the crystal structure, as well as the rigidity of the compound, are likely important to the potency of EPZ030456.

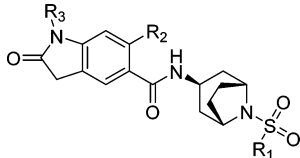
To understand further the inhibition of SMYD3 by EPZ030456 and EPZ031686, we determined their mechanism of action (MOA). Both compounds were essentially non-competitive with respect to both substrates. EPZ030456 is best described by mixed-type inhibition with respect to SAM with a  $K_i = 4.7 \pm 1.8 \text{ nM}$  and  $\alpha K_i = 1.1 \pm 0.1 \text{ nM}$  and is noncompetitive versus MEKK2 with a  $K_i = 1.3 \pm 0.1 \text{ nM}$

**Table 1. Piperidine Oxindole Compounds**

#	R1	R2	SMYD3 biochemical $IC_{50}$ (nM) <sup>a</sup>	SMYD3 ICW <sup>b</sup> $IC_{50}$ (nM) <sup>a</sup>
1	H	H	17000	>10000
2	SO <sub>2</sub> (CH <sub>2</sub> ) <sub>3</sub> NH <sub>2</sub>	H	160	>10000
3	SO <sub>2</sub> (CH <sub>2</sub> ) <sub>3</sub> NH <sub>2</sub>	Cl	80	6800
4	SO <sub>2</sub> -	H	70	>10000

<sup>a</sup> $IC_{50}$ s were determined from at least two independent experiments; see Supporting Information for details. <sup>b</sup>Trimethyl MEKK2 in Cell Western Assay; details in Supporting Information.

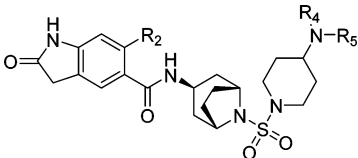
Table 2. Bridged Piperidine Sulfonamide Analogues



#	R1	R2	R3	cLogP	SMYD3 biochemical IC <sub>50</sub> (nM) <sup>a</sup>	SMYD3 ICW <sup>b</sup> IC <sub>50</sub> (nM) <sup>a</sup>
5		H	H	-0.32	4	3400
6		Cl	H	0.28	4	3200
7		H	H	0.06	1	480
8		H	Me	-0.46	26	3900
EPZ031686		Cl	H	2.18	3	36
9		Cl	H	0.03	2	760
10		Cl	H	0.32	5	730
11		Cl	H	0.32	4	1300
12		H	H	0.03	4	2200

<sup>a</sup>IC<sub>50</sub>s were determined from at least two independent experiments; see [Supporting Information](#) for details. <sup>b</sup>Trimethyl MEKK2 in Cell Western Assay; details in [Supporting Information](#).

Table 3. Bridged Piperidine Sulfamide Analogues



#	R2	R4	R5	cLogP	SMYD3 biochemical IC <sub>50</sub> (nM) <sup>a</sup>	SMYD3 ICW <sup>b</sup> IC <sub>50</sub> (nM) <sup>a</sup>
13	Cl	H	H	-0.77	1	1100
14	Cl	H	Me	-0.34	2	420
15	Cl	Me	Me	0.04	3	300
EPZ030456	Cl	H	Bn	1.38	4	48
16	F	H	H	-1.23	5	530
17	Me	H	H	-0.86	16	410
18	H	H	H	-1.38	1	850

<sup>a</sup>IC<sub>50</sub>s were determined from at least two independent experiments; see [Supporting Information](#) for details. <sup>b</sup>Trimethyl MEKK2 in Cell Western Assay; details in [Supporting Information](#).

(Supplementary Figure 2, Supplementary Table 1). EPZ031686 displays noncompetitive inhibition with respect to SAM and MEKK2 with a  $K_i = 1.2 \pm 0.1$  and  $1.1 \pm 0.1$  nM, respectively (Supplementary Figure 3, Supplementary Table 1). Observation of compound binding in the lysine pocket in the crystal structures suggests that these compounds would be

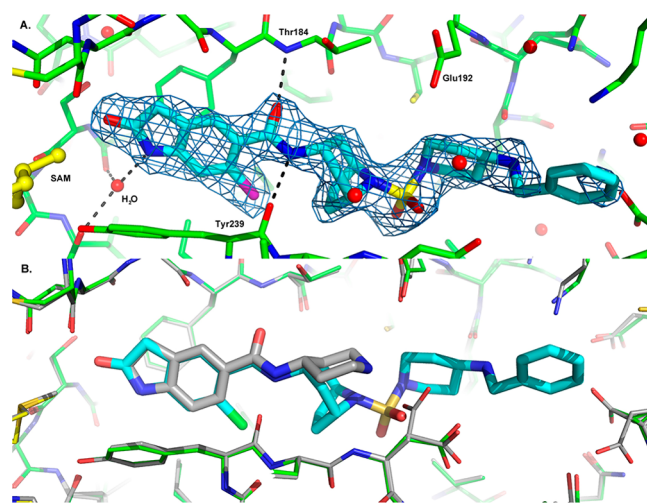


**Figure 2.** (A) Structure of EPZ030456 (cyan) with SMYD3 (green) and SAM (yellow) (PDB ID 5CCM). Electron density (2Fo-Fc, 1σ) for the compound is shown. Hydrogen bonds are indicated as dashed lines. (B) The headgroup of EPZ030456 (cyan) superimposes well with the oxindole of compound 1 (gray), while the saturated ring linkers take divergent paths in the active site.

competitive with respect to MEKK2; however, the observed mechanism is noncompetitive. We hypothesize that MEKK2 derives significant binding affinity from interactions with



SMYD3 outside of the lysine pocket (i.e., exosite binding) such that these small molecules cannot displace the protein substrate; noncompetitive inhibition by active site-directed small molecule inhibitors is a well established phenomenon for enzymes acting on macromolecular substrates.<sup>14</sup>

The two lead compounds were evaluated for *in vitro* metabolic stability and permeability to determine their suitability for *in vivo* PK determination. With a mean scaled clearance of 34 mL/min/kg in mouse liver microsomal incubations, EPZ030456 was slightly less stable than EPZ031686 (24 mL/min/kg). EPZ030456 also had a lower apical-to-basolateral apparent permeability ( $P_{app} = 0.34 \pm 0.22 \times 10^{-6}$  cm/s) in Caco-2 cells than EPZ031686 ( $P_{app} = 0.64 \pm 0.20 \times 10^{-6}$  cm/s). Both compounds were subject to active efflux in the Caco-2 cells, with efflux ratio values of 104 and 41, respectively. EPZ030456 and EPZ031686 had a free fraction of  $0.32 \pm 0.035$  and  $0.53 \pm 0.12$  in mouse plasma, respectively. Thus, overall, EPZ031686 had a more favorable *in vitro* ADME profile than EPZ030456.

Pharmacokinetic (PK) studies in CD-1 mice were performed by intravenous (i.v.) bolus and oral gavage (p.o.) administration. EPZ031686 blood PK parameters derived from noncompartmental analysis are displayed in Table 4. No

**Table 4. Pharmacokinetic Parameters for EPZ031686 Following i.v. and p.o. Bolus Administration to Male CD-1 Mice; Expressed as Mean  $\pm$  SD,  $n = 3$**

parameter	1 mg/kg i.v.	5 mg/kg p.o.	50 mg/kg p.o.
CL (mL/min/kg)	27 $\pm$ 3.9		
CL <sub>r</sub> (mL/min/kg)	5.3 $\pm$ 1.6		
V <sub>ss</sub> (L/kg)	2.3 $\pm$ 0.29		
t <sub>1/2</sub> (h)	1.7 $\pm$ 0.13	2.7 $\pm$ 0.98	2.2 $\pm$ 0.087
t <sub>max</sub> (h)		0.89 $\pm$ 0.19	1.3 $\pm$ 0.58
C <sub>max</sub> (ng/mL)		345 $\pm$ 89	4693 $\pm$ 826
AUC <sub>0-last</sub> (h·ng/mL)	603 $\pm$ 88	1281 $\pm$ 243	21158 $\pm$ 2517
AUC <sub>0-inf</sub> (h·ng/mL)	616 $\pm$ 90	1479 $\pm$ 167	21170 $\pm$ 2522
F (%)		48 $\pm$ 5.4	69 $\pm$ 8.2

significant blood to plasma partitioning was observed for this compound. Male mice administered a single dose of EPZ031686 at 1 mg/kg by i.v. bolus showed a moderate clearance (CL) of  $27 \pm 3.9$  mL/min/kg, in very good agreement with the mouse microsomal data, with a volume of distribution at steady state (V<sub>ss</sub>) of  $2.3 \pm 0.29$  L/kg, translating to a mean terminal half-life (t<sub>1/2</sub>) of  $1.7 \pm 0.13$  h. Approximately 20% of the administered dose was excreted unchanged in urine after 24 h, equivalent to a renal clearance (CL<sub>r</sub>) of  $5.3 \pm 1.6$  mL/min/kg. Following 5 and 50 mg/kg p.o. dosing, both C<sub>max</sub> and AUC<sub>0-last</sub> increased in a slightly higher than dose-proportional manner, while t<sub>1/2</sub> remained unchanged, suggesting a possible saturation of intestinal efflux. Bioavailability (F) of  $48 \pm 5.4\%$  and  $69 \pm 8.2\%$  was observed at 5 and 50 mg/kg, respectively, leading to EPZ031686 unbound blood concentration remaining above the SMYD3 IC<sub>50</sub> value for more than 12 h after a 50 mg/kg p.o. administration. In contrast, EPZ030456 solubility was not sufficient to be formulated for oral dosing at >30 mg/mL using a vehicle amenable to repeat dosing.

In conclusion, we report here the first potent, selective, small molecule SMYD3 inhibitors, sulfonamide EPZ031686 and sulfamide EPZ030456, with cellular potency suitable to probe the *in vitro* biology of SMYD3 inhibition. Further character-

ization of EPZ031686 showed it to have good bioavailability following oral dosing in mice making it a suitable tool for potential *in vivo* target validation studies.

## ■ ASSOCIATED CONTENT

### Supporting Information

The Supporting Information is available free of charge on the ACS Publications website at DOI: 10.1021/acsmchemlett.5b00272.

ADME/PK methods, cell assay conditions, biochemical assay conditions and MOA data, crystallography methods and data, synthesis and data for EPZ030456 and EPZ031686 (PDF)

## ■ AUTHOR INFORMATION

### Corresponding Author

\*E-mail: [lmitchell@epizyme.com](mailto:lmitchell@epizyme.com).

### Present Addresses

<sup>†</sup>Warp Drive Bio, 400 Technology Square, Cambridge, Massachusetts 02139, United States.

<sup>‡</sup>Genentech, Inc., 1 DNA Way, South San Francisco, California 94080, United States.

### Notes

The authors declare the following competing financial interest: L.H.M., P.A.B., S.S., M.T., N.R., C.K., J.T., T.V.R., A.R., S.L.J., M.F., N.J.W., K.W.K., R.A.B., J.J.S., and R.C. are employees and stockholders of Epizyme Inc.

## ■ REFERENCES

- (1) Vieira, F. Q.; Costa-Pinheiro, P.; Almeida-Rios, D.; Graca, I.; Monteiro-Reis, S.; Simoes-Sousa, S.; Carneiro, I.; Sousa, E. J.; Godinho, M. I.; Baltazar, F.; Henrique, R.; Jeronimo, C. SMYD3 contributes to a more aggressive phenotype of prostate cancer and targets Cyclin D2 through H4K20me3. *Oncotarget* **2015**, *6*, 13644.
- (2) Liu, Y.; Liu, H.; Luo, X.; Deng, J.; Pan, Y.; Liang, H. Overexpression of SMYD3 and matrix metalloproteinase-9 are associated with poor prognosis of patients with gastric cancer. *Tumor Biol.* **2015**, *36*, 4377.
- (3) Liu, Y.; Deng, J.; Luo, X.; Pan, Y.; Zhang, L.; Zhang, R.; Liang, H. Overexpression of SMYD3 was associated with increased STAT3 activation in gastric cancer. *Med. Oncol.* **2015**, *32* (1), 404.
- (4) Vieira, F. Q.; Costa-Pinheiro, P.; Ramalho-Carvalho, J.; Pereira, A.; Menezes, F. D.; Antunes, L.; Carneiro, I.; Oliveira, J.; Henrique, R.; Jeronimo, C. Deregulated expression of selected histone methylases and demethylases in prostate carcinoma. *Endocr.-Relat. Cancer* **2014**, *21* (1), 51–61.
- (5) Sponziello, M.; Durante, C.; Boichard, A.; Dima, M.; Puppini, C.; Verrienti, A.; Tamburrano, G.; Di Rocco, G.; Redler, A.; Lacroix, L.; Bidart, J. M.; Schlumberger, M.; Damante, G.; Russo, D.; Filetti, S. Epigenetic-related gene expression profile in medullary thyroid cancer revealed the overexpression of the histone methyltransferases EZH2 and SMYD3 in aggressive tumours. *Mol. Cell. Endocrinol.* **2014**, *392* (1–2), 8–13.
- (6) Liu, C.; Wang, C.; Wang, K.; Liu, L.; Shen, Q.; Yan, K.; Sun, X.; Chen, J.; Liu, J.; Ren, H.; Liu, H.; Xu, Z.; Hu, S.; Xu, D.; Fan, Y. SMYD3 as an oncogenic driver in prostate cancer by stimulation of androgen receptor transcription. *J. Natl. Cancer Inst.* **2013**, *105* (22), 1719–28.
- (7) Van Aller, G. S.; Reynoird, N.; Barbash, O.; Huddleston, M.; Liu, S.; Zmoos, A. F.; McDevitt, P.; Sinnamon, R.; Le, B.; Mas, G.; Annan, R.; Sage, J.; Garcia, B. A.; Tummino, P. J.; Gozani, O.; Kruger, R. G. Smyd3 regulates cancer cell phenotypes and catalyzes histone H4 lysine 5 methylation. *Epigenetics* **2012**, *7* (4), 340–3.

(8) Hamamoto, R.; Silva, F. P.; Tsuge, M.; Nishidate, T.; Katagiri, T.; Nakamura, Y.; Furukawa, Y. Enhanced SMYD3 expression is essential for the growth of breast cancer cells. *Cancer Sci.* **2006**, *97* (2), 113–8.

(9) Hamamoto, R.; Furukawa, Y.; Morita, M.; Iimura, Y.; Silva, F. P.; Li, M.; Yagyu, R.; Nakamura, Y. SMYD3 encodes a histone methyltransferase involved in the proliferation of cancer cells. *Nat. Cell Biol.* **2004**, *6* (8), 731–40.

(10) Liu, Y.; Luo, X.; Deng, J.; Pan, Y.; Zhang, L.; Liang, H. SMYD3 overexpression was a risk factor in the biological behavior and prognosis of gastric carcinoma. *Tumor Biol.* **2015**, *36* (4), 2685–94.

(11) Mazur, P. K.; Reynoird, N.; Khatri, P.; Jansen, P. W.; Wilkinson, A. W.; Liu, S.; Barbash, O.; Van Aller, G. S.; Huddleston, M.; Dhanak, D.; Tummino, P. J.; Kruger, R. G.; Garcia, B. A.; Butte, A. J.; Vermeulen, M.; Sage, J.; Gozani, O. SMYD3 links lysine methylation of MAP3K2 to Ras-driven cancer. *Nature* **2014**, *510* (7504), 283–7.

(12) Silva, F. P.; Hamamoto, R.; Kunizaki, M.; Tsuge, M.; Nakamura, Y.; Furukawa, Y. Enhanced methyltransferase activity of SMYD3 by the cleavage of its N-terminal region in human cancer cells. *Oncogene* **2008**, *27* (19), 2686–92.

(13) The 16 targets screened are DOT1L, EHMT1, EHMT2, EZH1, EZH2, NSD1, PRDM9, PRMT3, PRMT6, PRMT7, PRMT8, SETD7, SETDB1, SUV39H1, WHSC1, and WHSC1L1.

(14) Copeland, R. A. *Evaluation of Enzyme Inhibitors in Drug Discovery: A Guide for Medicinal Chemists and Pharmacologists*, 2nd ed.; Wiley: Hoboken, NJ, 2013.